

Spatially Extended Kondo State in Magnetic Molecules Induced by Interfacial Charge Transfer

U. G. E. Perera,¹ H. J. Kulik,² V. Iancu,¹ L. G. G. V. Dias da Silva,^{1,3} S. E. Ulloa,¹ N. Marzari,² and S.-W. Hla^{1,*}

¹*Department of Physics and Astronomy, Ohio University, Athens, Ohio 45701, USA*

²*Department of Materials Science and Engineering, MIT, Cambridge, Massachusetts 02139, USA*

³*Materials Science and Technology Division, Oak Ridge National Laboratory, Oak Ridge, Tennessee 37831, and Department of Physics and Astronomy, University of Tennessee, Knoxville, Tennessee 37996, USA*

(Received 6 June 2010; published 3 September 2010)

An extensive redistribution of spin density in TBrPP-Co molecules adsorbed on a Cu(111) surface is investigated by monitoring Kondo resonances at different locations on single molecules. Remarkably, the width of the Kondo resonance is found to be much larger on the organic ligands than on the central cobalt atom—reflecting enhanced spin-electron interactions on molecular orbitals. This unusual effect is explained by means of first-principles and numerical renormalization-group calculations highlighting the possibility to engineer spin polarization by exploiting interfacial charge transfer.

DOI: 10.1103/PhysRevLett.105.106601

PACS numbers: 72.15.Qm, 68.37.Ef, 75.20.Hr, 81.16.Dn

Molecular spintronics is an emergent field and a key challenge for future applications lies in probing and controlling the spin state of the molecules [1–16]. Recently, it was shown that charge-transfer processes can lead to the formation of novel states including magnetic [2], semi-conducting [17] and even superconducting [18] states. The Kondo effect, originated from a many body screening of a magnetic moment by host electrons, has been studied in several molecular systems [1–16,19]. However, the effect of organic ligands and interfacial charge transfer on the Kondo state are nontrivial, and critical questions remain unanswered. The Kondo temperature (T_K), a measure of spin-electron interaction strength, can be significantly higher for molecules [5,6,12–16] than magnetic atoms [7–11] on metal surfaces although these molecules host only one spin-active atom. In the gas phase, the TBrPP-Co [5, 10, 15, 20-Tetrakis-(4-bromophenyl)-porphyrin-cobalt] molecules have their spin mainly localized at the Co atom. Contrary to this we will show that an interfacial charge-transfer process dramatically alters the spin distribution of the molecule when it is adsorbed on a Cu(111) surface and the entire molecule becomes spin active. This is a direct consequence of the ligands acquiring a spin polarization in competition with the spin density of the metal center.

The TBrPP-Co adsorbed on Cu(111) [6,15] is an excellent model system to investigate spin polarization, the effect of molecular orbitals in the Kondo state, and interfacial charge-transfer processes. TBrPP-Co has a porphyrin unit with a cobalt (Co) atom caged at its center [Fig. 1(a)]. The experiments were conducted using a custom-built low-temperature scanning tunneling microscope (STM) system operated in pressures below 4×10^{-11} Torr and at 6 K. The Cu(111) sample was cleaned by repeated cycles of Ne ion sputtering and annealing to 800 K. A submonolayer coverage of TBrPP-Co was vacuum deposited on a clean Cu(111) surface held at ~ 120 K that was further cooled to 6 K for measurements.

STM images [Fig. 1(b)] show the TBrPP-Co molecules on Cu(111) with four pronounced lobes. The TBrPP-Co is positioned on Cu(111) with its central Co atom directly located on top of a surface Cu atom and forms ordered ribbonlike islands [20]. The Kondo state of the molecules can be directly probed via dI/dV tunneling spectroscopy, which reveals a prominent feature near zero bias. The dI/dV tunneling spectroscopy and spectroscopic images are recorded with a lock-in amplifier by adding a 1 mV ac modulation at 720 Hz. The measured Kondo resonances are fitted by the Ujsaghy's formula [19]. The T_K at the center of a TBrPP-Co inside a self-assembled molecular layer is ~ 105 K [6]. Intuitively, one would expect the Kondo resonance to be stronger at the Co atom location because it is the only spin-active atom caged in the molecule. Surprisingly, we observe the Kondo resonance not only at the center but also throughout the entire porphyrin ring. This is confirmed unequivocally by a Kondo map (dI/dV image, Fig. 2) acquired at a 5 mV energy window. The dI/dV data reveal the Kondo state as a dip at $\sim \pm 25$ mV around the Fermi level. Accordingly, the spectroscopic image shows a depression in the two dimensional spectral region over which the Kondo signature is observed. The blue and black regions in Fig. 2(b) represent the Kondo map of a molecule inside a molecular layer, associated with the simultaneously acquired STM image [Fig. 2(a)]. The change in contrast, i.e., blue and black, is due to the variation of the dI/dV curve slope and it does not necessarily represent the changes in T_k . To accurately measure the T_K at each location, it is imperative to acquire a full spectrum (Fig. 3). The dI/dV map in Fig. 2(b) clearly reveals that the entire porphyrin exhibits a Kondo signal. It is worth noting that a similar phenomenon is observed in isolated molecules on Cu(111) [20] and thus the observed Kondo phenomenon is driven by the molecule-substrate interactions, rather than by in-plane molecular interactions from self-organization.

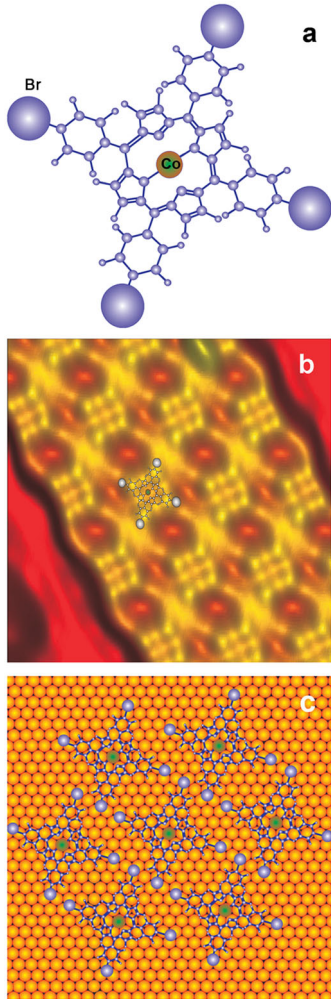


FIG. 1 (color online). Molecular self-assembly. (a) Chemical structure of TBrPP-Co, (b) an STM image of a self-assembled TBrPP-Co on Cu(111) [1 V, 1.3 nA, $6.3 \times 5.6 \text{ nm}^2$], and (c) the adsorption model of the molecules.

The variation of T_K across the molecule is clearly evident from the tunneling spectroscopy data measured along two outward paths; a diagonal (path 1, towards a bromophenyl unit) and across the molecule (path 2, along a Co-N bond), starting from the molecule center [Fig. 3(a)]. These dI/dV spectra reveal the Kondo resonance to have higher T_K values on the ring than at the center of the molecule [Fig. 3(b) and 3(c)]. The T_K increases from $108 \pm 5 \text{ K}$ to $212 \pm 6 \text{ K}$ for path 1, and from $107 \pm 4 \text{ K}$ to $149 \pm 3 \text{ K}$ for path 2 as the tip is moved away from the molecule center [Fig. 3(d)]. Remarkably, the highest T_K is found when the STM tip is located over a protruding lobe of the molecule, i.e., near a bromophenyl unit.

To understand the varied Kondo resonance across the molecule, we perform density functional theory (DFT) calculations [21] using the Perdew-Burke-Ernzerhof scheme [22]. In addition, a Hubbard-like potential energy term [23,24] is employed, which can greatly improve DFT descriptions of the transition-metal complexes [25–27]. A periodic boundary condition, plane wave basis, and an

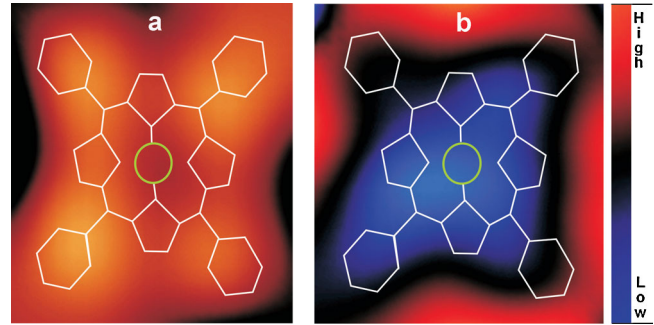


FIG. 2 (color online). Kondo map. (a) STM image showing a TBrPP-Co molecule inside a SAM. (b) The Kondo map (dI/dV spectroscopic image) of the molecule acquired with 5 mV bias [$1.3 \times 1.6 \text{ nm}^2$]. The black and blue region indicates the Kondo effect, which extends over the entire porphyrin molecule. A molecular drawing is added on top of the image for eye guidance.

ultrasoft pseudopotential code are used for the computations. The pseudopotentials include both $3d$ and $4s$ orbitals in the valence for the Co and Cu. In both cases, the Hubbard U is determined from a self-consistent linear-response procedure on the full system [25,26]; the calculated values for both gas-phase and adsorbed molecules are quite similar at 4.9 and 5.4 eV, respectively. We optimize the structures of both the isolated TBrPP-[Co,Cu] and the molecule-Cu(111) slab complexes. In the gas phase, the phenyl rings are constrained to lie in the plane of the porphyrin base to facilitate comparison to the molecule-slab complex, where a planar molecule geometry is preferred. For the molecule-Cu(111) slab, both the molecule and its relative distance to the surface (on average 2.5 \AA) are optimized. The geometry optimization also allows the molecule to laterally adjust on Cu(111) and the most optimum geometry is achieved when the Co atom is located on top of a surface Cu atom (Fig. 4). Thus, the DFT result independently confirms the experimental adsorption geometry [20].

In the gas phase, the TBrPP-Co molecule has its spin density localized at the $3d^7$ Co(II) center (magnetic moment; $1.08 \mu_B$) as expected [Fig. 4(a)]. However, when the molecule is adsorbed on the Cu(111) surface, the spin density delocalizes over the entire molecule with an actual decrease at the Co site, which becomes a $3d^8$ Co(I) state (magnetic moment; $0.06 \mu_B$). Now, the sites of greatest spin density in the molecule become the carbon atoms that connect to the bromophenyls [Fig. 4(b)], while portions of the pyrrole groups still exhibit spin densities about half as large. Interestingly, the calculations also reveal a sizeable charge transfer from the surface to the molecule [Fig. 4(c)]. The amount of charge transfer is estimated from Löwdin-charge differences, with a net charge increase in the molecule upon complexation of ~ 2.25 electrons from the surface (~ 0.5 electrons to the Co and ~ 1.75 electrons distributing throughout the ring). The parts of the underlying surface that exhibit greatest charge depletion are the sites under the Co and those along the directions towards the pyrrole groups [Fig. 4(c)]. On the molecule, the greatest

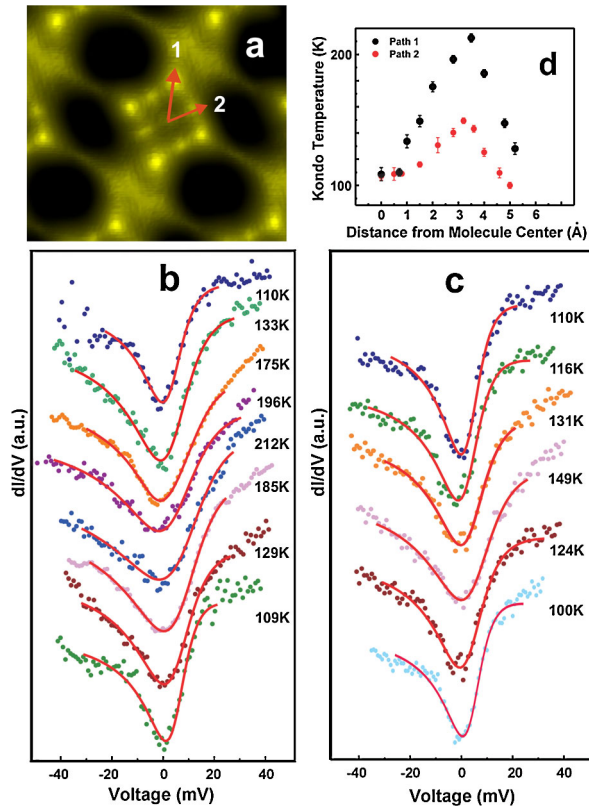


FIG. 3 (color online). Kondo temperature across the molecule. (a) The arrows 1 and 2 indicate the paths along which the Kondo signatures are recorded [$3.8 \times 3.2 \text{ nm}^2$]. (b),(c) Sequences of Kondo resonances recorded along paths 1 and 2, respectively. The spectra from top to bottom are measured from the center towards the edge and are vertically and horizontally displaced for clarity. The solid line represents the Fano line-shape fit to the experimental data. (d) Kondo temperature versus distance from the center of the molecule for both paths. Error bars are produced from the statistical distribution of measured data on different molecules with different tips (separate experimental runs). Each data point here is an average between 8 to 20 curves.

charge increase is seen along the outer porphyrin edge, while the bromines are the only atoms that exhibit a slight depletion in charge upon complexation.

In principle, charge transfer from the surface to the porphyrin should also occur in a similar molecule, TBrPP-Cu on Cu(111), where the central Co is replaced with a Cu atom. However, previous experiments [6,15] did not observe Kondo features in this system. For comparison, GGA + U calculations for the TBrPP-Cu on a Cu(111) are performed as well. We find that the majority of the $3d$ -derived molecular orbitals of the $3d^9$ Cu(II) are located well below the surface Fermi level with the exception of a single $3d_{x^2-y^2}$ molecular orbital for the minority spin, which lies above the Fermi energy [Fig. 4(e)] [20]. For TBrPP-Co, the Cu(111) atoms in the axial position stabilize the double occupation of a $3d_z^2$ orbital that is located close to the surface Fermi level and has a maximal overlap with the surface. Charge transfer to the molecule causes the

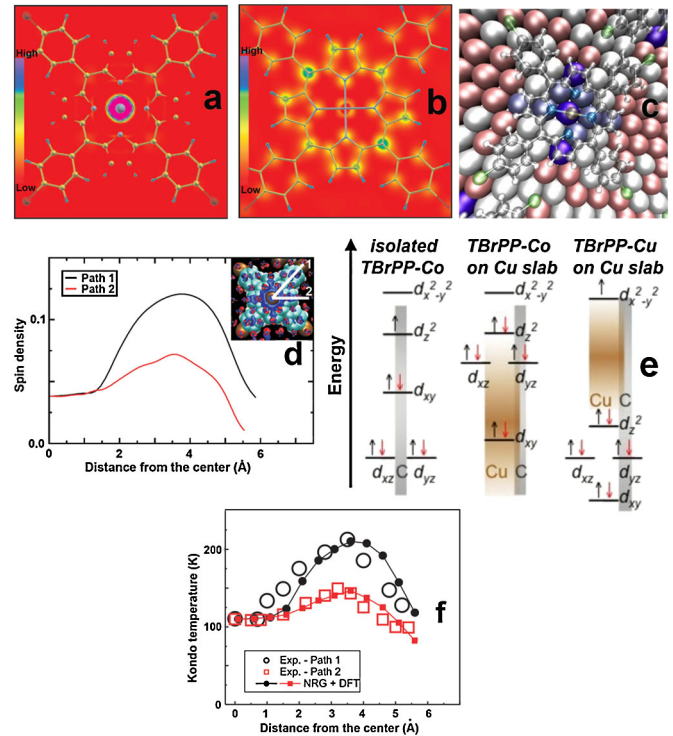


FIG. 4 (color online). Calculated spin density and Kondo temperature. (a) A gas phase TBrPP-Co has its spin concentrated at a central Co atom. (b) TBrPP-Co on a Cu(111) surface reveals its spin density spreads over the entire porphyrin ring. (c) A perspective view of TBrPP-Co on Cu(111) showing the extent of charge transfer from surface Cu atoms to the molecule (blue: highest, grey: medium, and red; the smallest charge transfer). (d) Calculated spin density averaged over paths 1 and 2 (shown in inset). (e) Illustration of $3d$ states where the total occupied carbon-derived states of the molecule (grey) and the occupied bulk Cu states (brown) are indicated by shaded regions. (f) Kondo temperature extracted from the DFT total spin density in Fig. 4(d) and the NRG calculation shows excellent agreement with experimental data for both paths.

change in the ligand field that induces a transition from $3d^7$ Co(II) to $3d^8$ Co(I). It also causes the reorganization of the spin density, which is initially localized on the doublet Co (II) center, to delocalize and distribute throughout the porphyrin ring.

The calculated spin densities along the two paths where the T_K values are obtained [Fig. 4(d)] reveal similar trends as in experiment [Fig. 3(d)]: They increase toward the edge of the molecule and then drop passing the edge. Furthermore, the spin density along path 1 is higher than that of path 2, as in the experiment [Fig. 3(d)]. Since T_K depends on the host density of states “ ρ ” and spin-electron coupling “ J ” as $k_B T_K \propto e^{-1/\rho J}$, the variation in spin density will vary the spin-electron coupling J , and so the T_K will vary accordingly. A quantitative correlation of T_K to the spin density can be extracted utilizing numerical renormalization-group (NRG) method [28,29]. Our NRG calculations take into account the delocalized molecular

spin obtained from the DFT calculation and also incorporate the integrated densities. This provides an interesting scenario for Kondo physics, as the typical situation is that the magnetic moment of the Kondo impurity resides in a pointlike object. Here, the large molecule extends over several surface atoms, and the variation of the spin density at different locations on the molecule correlates with changes in T_K across it. Although NRG calculations of T_K in porphyrins have found variations with charge transfer [30], the detailed analysis of the spatial dependence seen by STM is beyond the scope of such treatment. Here we use a model where the spatial variation of the Kondo screening is associated with a position-dependent effective antiferromagnetic exchange coupling $J(x)$ between the surface and the molecule. Although $J(x)$ can be written as an exchange integral between metallic and unfilled d -like states (and therefore is implicitly associated with the spin density) a detailed derivation of $J(x)$ from first-principles is numerically demanding and lies beyond the scope of this work. Instead, guided by the DFT calculations, we assume the system can be described by an effective single-channel spin-1/2 Kondo model where the exchange coupling is modulated by the spin density as $J(x) = J_0 + An_{\text{DFT}}(x)$. Here, J_0 and A are the fitting parameters, and $n_{\text{DFT}}(x)$ is shown in Fig. 4(d). Using $J(x)$ as an input, T_K is obtained from NRG magnetic susceptibility curves assuming a constant metallic density of states [28]: $\rho = (2D)^{-1}$. The band-discretization parameter (Λ) is fixed at $\Lambda = 2.5$, and up to 1000 states are kept on each NRG iteration. We obtain $\rho A = 0.2$, $\rho J_0 = 0.15$, and for a characteristic Cu half bandwidth, $D = 11$ eV. This two-parameter fit is able to describe the entire data set. The resulting position-dependent T_K values are consistent with the experimental measurements [Fig. 4(g)] thereby conforming the DFT results. This excellent quantitative agreement supports the conclusion of T_K increasing over the porphyrin as the direct result of the enhanced spin density in the molecular orbital.

In summary, we show that the spin polarization in a metallo-porphyrin (TBrPP-Co) can drastically change due to an interfacial charge transfer after molecular adsorption on a metal surface, where the macrocycle ring becomes spin active. This finding further illustrates that the interfacial charge transfer can dramatically affect the magnetic behavior of molecules, which could be used to tailor novel molecular complexes for future spintronic applications including spin injection and spin filtering processes. This work also paves the way for other experiments like x-ray absorption spectroscopy (XAS) and x-ray magnetic circular dichroism (XMCD) to study the magnetism of this molecular system.

We acknowledge financial support from the U.S. Department of Energy, BES grant DE-FG02-02ER46012, NSF-PIRE-OISE 0730257, NSF-WMN 07010581, NSF-DMR 0706020, and ARO-MURI DAAD-19-03-1-0169 (H.J.K., N.M.). Computational facilities were provided through the PNNL Grant No. EMSL-UP-9597.

*Corresponding author.

hla@ohio.edu; url: www.phy.ohiou.edu/~hla

- [1] D. Wegner *et al.*, *Phys. Rev. Lett.* **103**, 087205 (2009).
- [2] I. Fernandez-Torrente, K. J. Franke, and J. I. Pascual, *Phys. Rev. Lett.* **101**, 217203 (2008).
- [3] C. Iacovita *et al.*, *Phys. Rev. Lett.* **101**, 116602 (2008).
- [4] G. Chiappe and E. Louis, *Phys. Rev. Lett.* **97**, 076806 (2006).
- [5] A. D. Zhao, Z. Hu, B. Wang, X. Xiao, J. Yang, and J. G. Hou, *J. Chem. Phys.* **128**, 234705 (2008).
- [6] V. Iancu, A. Deshpande, and S.-W. Hla, *Phys. Rev. Lett.* **97**, 266603 (2006).
- [7] V. Madhavan, W. Chen, T. Jamneala, M. F. Crommie, and N. S. Wingreen, *Science* **280**, 567 (1998).
- [8] J. Li, W.-D. Schneider, R. Berndt, and B. Delley, *Phys. Rev. Lett.* **80**, 2893 (1998).
- [9] N. Knorr, M. A. Schneider, L. Diekhoner, P. Wahl, and K. Kern, *Phys. Rev. Lett.* **88**, 096804 (2002).
- [10] T. Uchihashi, J. W. Zhang, J. Kroger, and R. Berndt, *Phys. Rev. B* **78**, 033402 (2008).
- [11] J. Henzl and K. Morgenstern, *Phys. Rev. Lett.* **98**, 266601 (2007).
- [12] A. D. Zhao *et al.*, *Science* **309**, 1542 (2005).
- [13] L. Gao *et al.*, *Phys. Rev. Lett.* **99**, 106402 (2007).
- [14] Y.-S. Fu *et al.*, *Phys. Rev. Lett.* **99**, 256601 (2007).
- [15] V. Iancu, A. Deshpande, and S.-W. Hla, *Nano Lett.* **6**, 820 (2006).
- [16] P. Wahl, L. Diekhöner, G. Wittich, L. Vitali, M. A. Schneider, and K. Kern, *Phys. Rev. Lett.* **95**, 166601 (2005).
- [17] F. Jackel, U. G. E. Perera, V. Iancu, K.-F. Braun, N. Koch, J. P. Rabe, and S.-W. Hla, *Phys. Rev. Lett.* **100**, 126102 (2008).
- [18] K. Clark, A. Hassanien, S. Khan, K.-F. Braun, H. Tanaka, and S.-W. Hla, *Nature Nanotech.* **5**, 261 (2010).
- [19] O. Ujsaghy, J. Kroha, L. Szunyogh, and A. Zawadowski, *Phys. Rev. Lett.* **85**, 2557 (2000).
- [20] See supplementary material at <http://link.aps.org/supplemental/10.1103/PhysRevLett.105.106601>.
- [21] P. Giannozzi *et al.*, *J. Phys. Condens. Matter* **21**, 395502 (2009).
- [22] J. P. Perdew, K. Burke, and M. Ernzerhof, *Phys. Rev. Lett.* **77**, 3865 (1996).
- [23] V. I. Anisimov, J. Zaanen, and O. K. Andersen, *Phys. Rev. B* **44**, 943 (1991).
- [24] A. I. Liechtenstein, V. I. Anisimov, and J. Zaanen, *Phys. Rev. B* **52**, R5467 (1995).
- [25] M. Cococcioni and S. de Gironcoli, *Phys. Rev. B* **71**, 035105 (2005).
- [26] H. J. Kulik, M. Cococcioni, D. A. Scherlis, and N. Marzari, *Phys. Rev. Lett.* **97**, 103001 (2006).
- [27] H. J. Kulik and N. Marzari, *J. Chem. Phys.* **129**, 134314 (2008).
- [28] R. Bulla, T. A. Costi, and T. Pruschke, *Rev. Mod. Phys.* **80**, 395 (2008).
- [29] R. Temirov, A. Lassise, F. B. Anders, and F. S. Tautz, *Nanotechnology* **19**, 065401 (2008).
- [30] L. G. G. V. Dias da Silva, M. L. Tiago, S. E. Ulloa, F. A. Reboredo, and E. Dagotto, *Phys. Rev. B* **80**, 155443 (2009).